Electronic Supplementary Material (ESI) for Journal of Materials Chemistry B.

A mimotope peptide-based dual-signal readout competitive enzyme-linked immunoassay for non-toxic detection of Zearalenone

Yanjie Chen[a], Shupei Zhang[b], Zhensheng Hong[a], Yanyu Lin[c], Hong Dai[a,b*]

a College of Chemistry and Materials, Fujian Normal University, Fuzhou 350108, P. R. China

b Fujian Provincial Maternity and Children`s Hospital, Fuzhou, Fujian, 350108,China

c Ministry of Education Key Laboratory of Analysis and Detection for Food Safety, and Department of Chemistry, Fuzhou University, Fuzhou 350002, P. R. China

Corresponding author: Fax: (+86)-591-22866135; E-mail: dhong@fjnu.edu.cn (H. Dai);

Table S1

Recovery measurments of ZEN in soy sauce (n=3)

Smple	Found (ng/mL)	Add (ng/mL)	Total found (ng/mL)	Recovery (%)
1	0.0549	blank	0.0549	
2	0.0549	0.1	0.1542	99.3
3	0.0549	0.01	0.0654	104.7
4	0.0549	0.001	0.05595	105.1

Synthesis of Au nanocones

In order to harvest pure Au nanocones (Au NCs), we took Li's work as reference with some minor modifications.[24] In particular, 250 μL of 0.01M $HAuCl_4$ solution and 250 μL of 0.01M H_2PtCl_6 solution were mixed together at room temperature and added to 20 mL 0.1 M CTAB solution under stirring. Next, 2 mL new prepared $NaBH_4$ ice-cold solution (0.01M) was injected into the mixture slowly and shook for 5 min followed by keeping in an oven at 35 ℃ for 5 h to acquire the seed solution. Besides, a mixture composited of 3.5 mL $HAuCl_4$ (0.01M), 150 μL H_2PtCl_6 (0.01M), 800 μL $AgNO_3$ (0.01M) and 1600 μL HCl (1M) was added into 80mL of 0.1 M CTAB solution and vigorously stirred for 5 min to get uniform solution. After that, 640 μL of 0.1 M ascorbic acid (AA) solution was injected into the mixed solution under stirring to have a reduce reaction. When the mixed solution changed to colorless, the seed solution prepared above was added immediately and vigorously stirred for 5 min. After that, the mixture was put into oven to have a constant temperature reaction at 35 ℃ for 12 hours. The Au NCs solution was purified just by centrifuging (6000 r/min, 10 min) to remove the solid from the supernatant. Finally, the prepared Au NCs was functionalized with 1mg mL^{-1} MEA under volume ratio of 1:3 and stirred for 6 h. The MEA could connected to Au NCs via formation of Au-S bond.

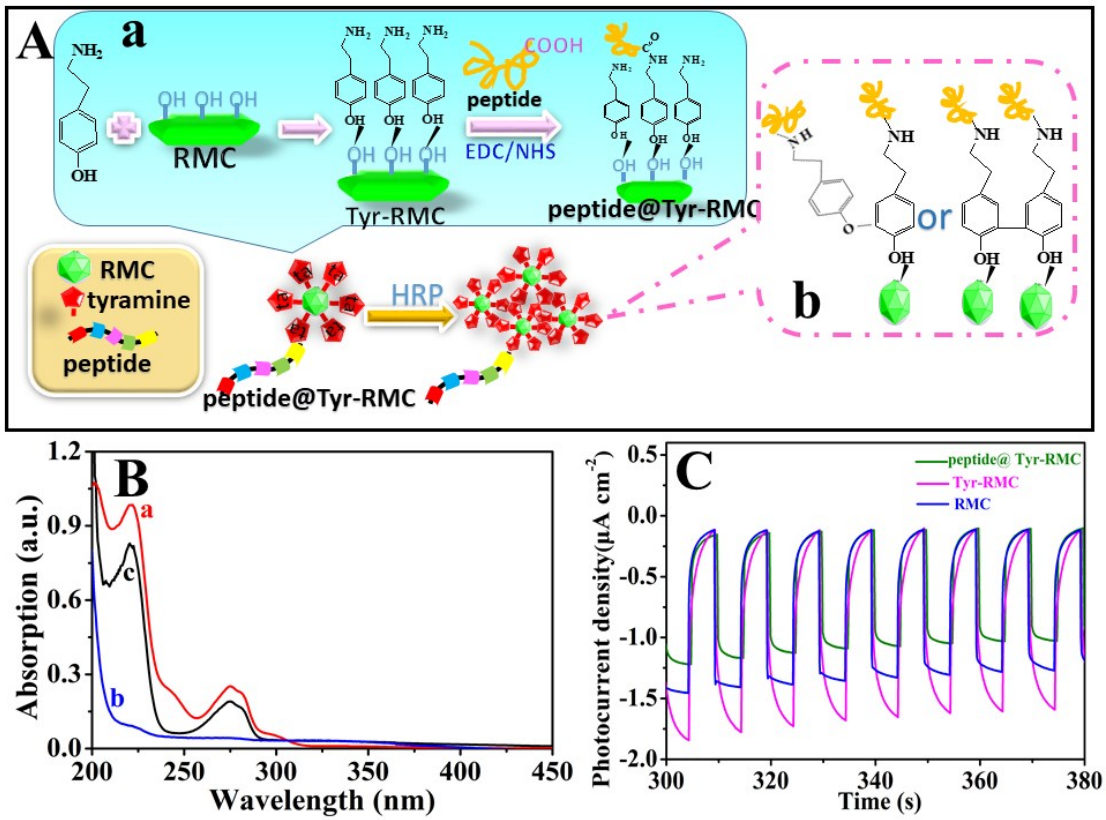

Figure S1 (A) The illustration of the construction process of peptide@Tyr-RMC. (B) Absorbance spectra of tyramine (a), RMC (b), ta-RMC (c). (C) Photocurrent density measurement on different modified electrode RMC (blue line), Tyr-RMC (magenta line) and peptide@Tyr-RMC (green line) in PBS (pH 7.0) with applied potential of 0.2V.

Fig. S1A (a) described the construction process of peptide@Tyr-RMC. The oxygen vacancies in RMC trended to capture H_2O molecules and H_2O molecules dissociated into OH and H fragments, thereby caused formation of Ti-OH on RMC surface. In this case, hydroxyl in tyramine was prior to connect onto RMC surface via hydrogen bond between hydroxyl and Ti-OH.[32] After introduction of ZMP, the mimotope peptide connected to Tyr-RMC via classic EDC/NHS coupling reaction between amine ($-NH_2$) groups on tyramine and carboxyl (-COOH) group of peptide.[33,34] As for Fig. S1A (b)

described the signal amplification mechanism of peptide@Tyr-RMC composite. Subjecting to catalytic of HRP, ta-RMC composite depose at the site of enzyme reaction through either a C–C linkage between the other-carbons of the aromatic ring or a C–O linkage between the ortho-carbon and the phenolic oxygen[36-38]. To verify the successful preparation of Tyr-RMC composite optical properties of obtained pure and doped systems were recorded by ultraviolet-visible absorption spectra (UV-vis) in Fig. S1B. As exhibited in Fig. S1B, the unmodified RMC (b) did not show apparent UV light absorption in wavelength range from 200 nm to 450 nm because of its wide band gap[S1]. While pure tyramine (a) indicated an evident absorption peak at 225 nm and 275 nm, which was correspond to previous reports[38]. After modifying RMC with tyramine, the Tyr-RMC composite (c) showed the characteristic absorption peaks of both 225 nm and 275 nm, indicating that tyramine have successfully coated on the RMC surface. To further verified that the peptide@Tyr-RMC composite (green line) was successfully synthesized, the photocurrent response on different composite modified electrode were evaluated in Fig. S1C. Comparing with unmodified RMC (blue line), the Tyr-RMC composite (magenta line) presented increasing photocurrent response owing to self-oxidization of tyramine suppressed the recombination of electron-hole pairs in RMC. Whereas as peptide@Tyr-RMC composite anchored onto the electrode, the photocurrent response decreased for insulated protein complex inhibited the electron transfer. Based on these discussions we can infer that the peptide@Tyr-RMC probe has successfully fabricated.

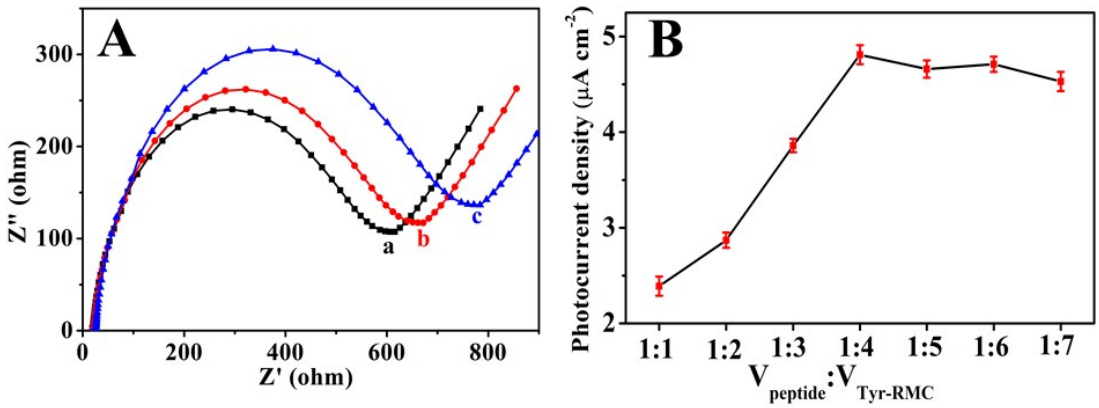

Figure S2 (A) EIS and measurement on different modified electrode (a) GCE/CNHs/ Au NCs/poly (Gly) /Ab, (b) GCE/CNH/Au NCs/poly (Gly)/Ab/peptide, (c) GCE/CNH/Au NCs/ poly (Gly)/Ab/peptide@Tyr-RMC (B) Photocurrent response on GCE/CNH/Au NCs/poly (Gly)/Ab/ peptide@Tyr-RMC under different volume ratio between peptide and Tyr-RMC

As illustrated in Fig.S2A, the electrochemical impedance on GCE/CNH/Au NCs/poly (Gly)/Ab/mimotope peptide (curve b) was evidently larger than that on GCE/CNH/Au NCs/poly (Gly)/Ab (curve a), implying that an immune recognition reaction took place between mimotope peptide and antibody. After peptide@Tyr-RMC immobilized on GCE/CNH/Au NCs/poly (Gly)/Ab electrode, electrochemical impedance on GCE/CNH/Au NCs/poly (Gly)/Ab/peptide@Tyr-RMC (curve c) was remarkably increased comparing to curve **a** and **b**. Therefore, we drawed a conclusion that the peptide@Tyr-RMC could still recognize the antibody on GCE/CNH/Au NCs/poly (Gly)/Ab electrode even though Tyr-RMC attached, which also indicated that the Tyr-RMC as a report unit played an important role in signal amplification. To specially explore the interaction between antibody and peptide@Tyr-RMC, Fig. S2B presented the photocurrent response on GCE/CNH/Au NCs/ poly (Gly)/Ab electrode after

incubating with peptide@Tyr-RMC probe with different volume ratio between mimotope peptide and Tyr-RMC. The photocurrent density increased hugely with increased ratio of Tyr-RMC in the range from 1:1 to 1:4 and the maximum photocurrent density value appeared at ratio of 1:4, whereas the photocurrent trended to level off and decline after 1:4. For one thing, the adsorption between Tyr-RMC and mimotope peptide was saturated. For another, RMC aggregated at excess volume ratio and part of mimotope peptide was coated by Tyr-RMC, which inhibited the interaction with antibody on electrode interface. Therefore, 1:4 was finally selected as the optimal volume ratio between mimotope peptide and Tyr-RMC.

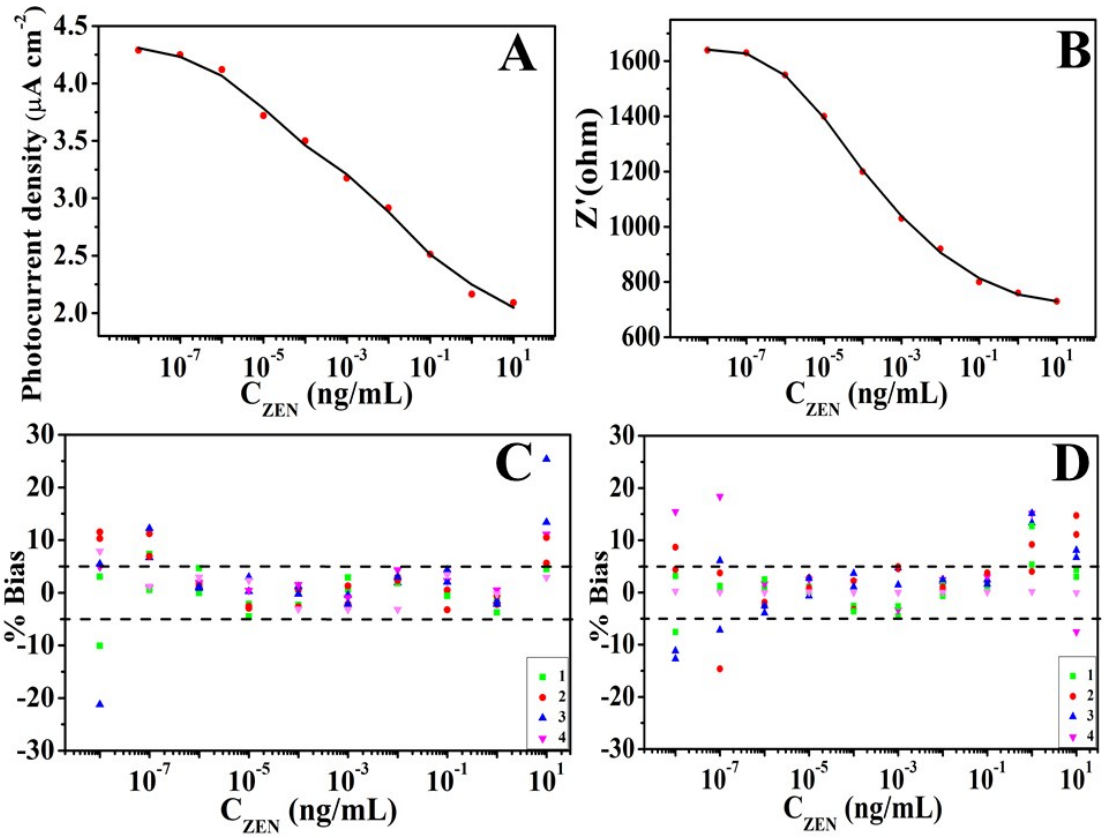

Figure S3 LBA curves of photocurrent response (A) and electrochemical impedance measurement (B) for different concentration of ZEN after treating with 0.5 mg mL $^{-1}$ HRP. %Bias plots for photocurrent response (C) and electrochemical impedance measurement (D) by preparing four independent sets of mock standards to have two analysts prepare two sets each

Considering that this is a competitive assay, the instrument response was inversely related to the analyte concentration in ligand binding assay (LBA).[35] While the non-linear nature of an LBA curve limits the concentration response correlation at the upper and lower ends of the curve, resulting in plateaus and therefore an S-shaped curve, as presented in Fig.S3 A and B. In this case, the concentration-response relationship of these calibrator standards established the calibration curve of the assay. The % bias plots was practical approach to establish the quantitation range and to judge the usefulness of auxiliary points. As illustrated in Fig. S3 C and D, four independent sets of mock standards was prepared to have two analysts prepare two sets each and each

set of mock standards was added to an assay plate in duplicate wells. The %bias used in the example was as follows:

$$\%Bias = \frac{Determined\ Concentration - Normal\ concentration}{Normal\ concentration} \times 100\%$$

According to guidance, bias of up to 25% at the LLOQ level was acceptable. While to purse a tighter bias acceptance standards with bias less than 5% seem to make a suitable quantification range in the example provided here. The % bias plots in Fig. S2C and D indicated that the quantification range (LLOQ to ULOQ) for photocurrent and electrochemical impedance measurement should be 10^{-6} to 1 ng/mL and 10^{-6} to 10^{-1} ng/mL respectively. Based on this, the S-shaped curves in Fig. S2A and B were fitted into standard curves in effective liner range as presented in Fig.4B and D. The linear regression equation of two curves were expressed as Photocurrent density ($\mu A\ cm^{-2}$) = $-0.318 \log C_{ZEN}$ (ng/mL) + 1.99 (R^2 = 0.9987) and Z' (ohm) = $-152.93 \log C_{ZEN}$ (ng/mL) + 620.30 (R^2 = 0.9911) respectively. And loss of linearity indicated that the assay has reached its limits of the detection, thus, the detection limit for the designed biosensor was 10^{-6} ng/mL.

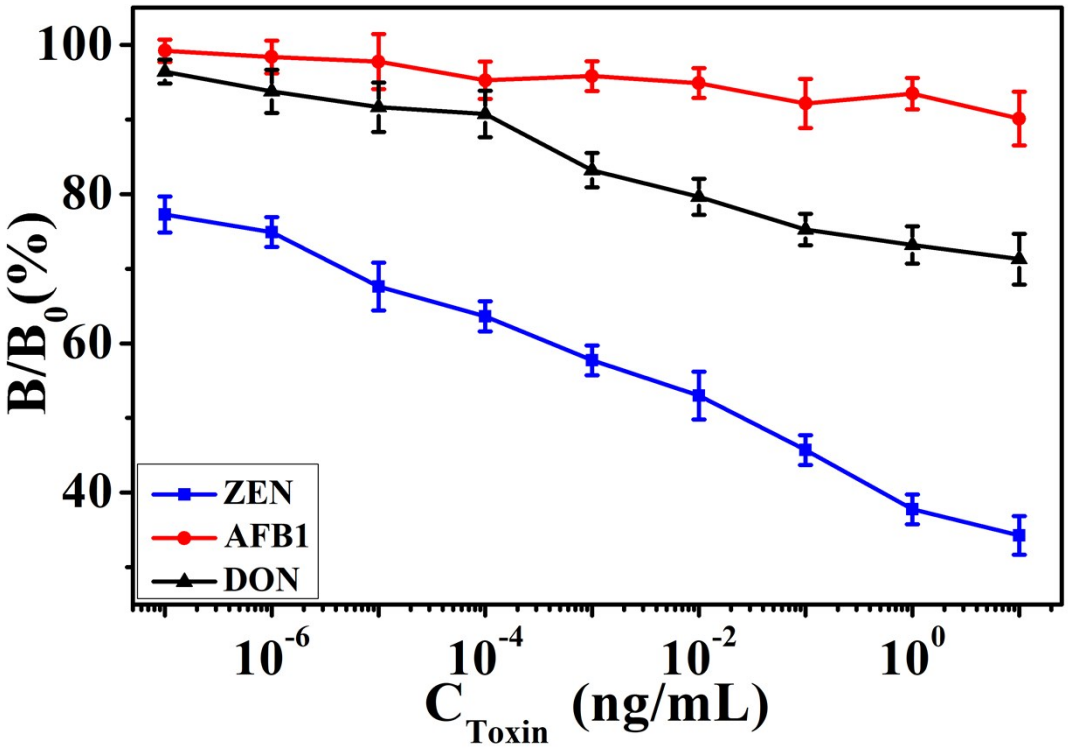

Figure S 4 The competitive inhibition curves of competitive ELISA with ZEN, AFB1 and DON from 10^{-7} ng/mL to 10 ng/mL.

To further test the specify of designed immunoassay, the competitive inhibition curves of ZEN, AFB1 and DON were established in Fig. S4. The B_0 was the binding signal when competitive antigen concentration was 0 ng/mL and B was the binding signal when the competitive antigen at other concentrations. The half maximal (50%) inhibitory concentrations (IC50) represented the concentration of an inhibitor with 50% inhibition ratio (B/B_0) of antibody. In common, a lower IC50 implied a better specified ability of antibody. The half maximal (50%) inhibitory concentrations (IC50) of ZEN was calculated to be 0.0144 ng/mL. And IC50 of AFB1 and DON were both greater than the highest concentration in standard curve (1 ng/ mL). Furthermore, IC50 of DON seems to be lower than of AFB1, implying the ZEN antibody demonstrated a relative lower specify ability to DON compare to AFB1[40]. This conclusion can well explain the

phenomenon in Fig. 5A and C.

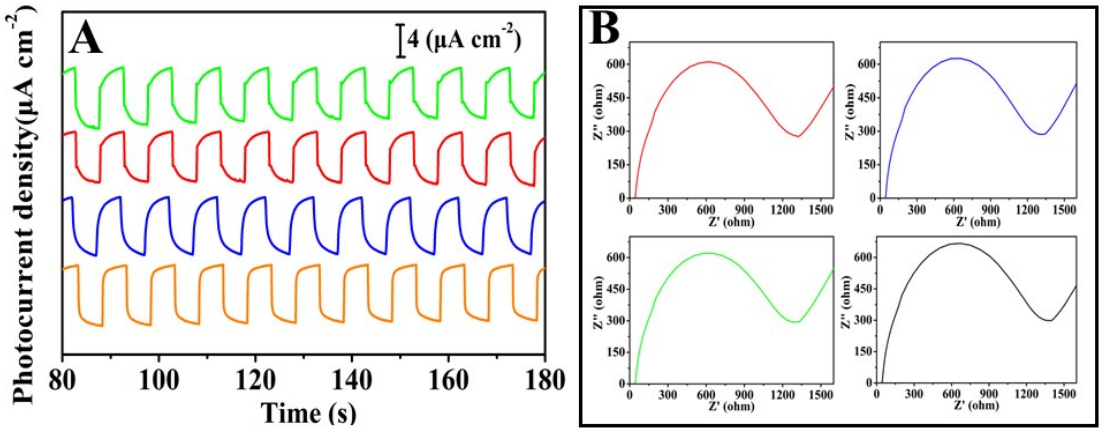

Figure S5 The reproducibility of PEC biosensor was evaluated by determining photocurrent response in four electrodes (GCE/CNH/Au NCs/poly (Gly)/Ab/ peptide@ta-RMC /HRP-H_2O_2) under chopped light illumination with applied potential of 0.2V in PBS (pH 7.0) (A). And EIS in four electrodes (GCE/CNH/Au NCs/poly (Gly)/Ab/peptide@ta-RMC/HRP-H_2O_2) in mixed solution of 5.0 mM $K_3[Fe(CN)_6]/K_4[Fe(CN)_6]$ (1:1) contained 0.5 M KCl with applied potential of 0.199V (B).

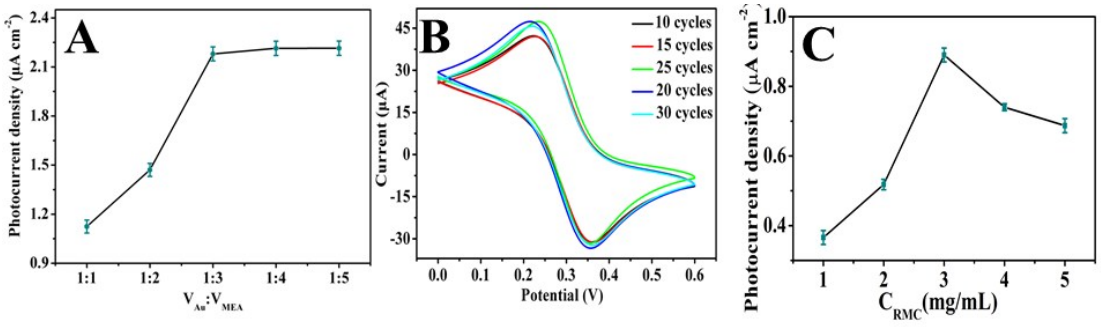

Figure S6 effect of (A) volume ratio between Au CNs and MEA, (B) different electrochemical polymerization cycle of Glycine on electrode interface, (C) different concentration of RMC, (D) volume ratio between peptide and Tyr-RMC.

The influence of volume ratio between Au NCs and MEA was analyzed in Fig. S6A, the Au NCs was compound with MEA under the volume ratio of 1:1, 1:2, 1:3, 1:4 and 1:5 respectively, with increasing volume ratio, the photocurrent enhanced rapidly and level off at 1:3. After that, more MEA absorbed on the surface of Au NCs via Au-S bond, the steric hindrance generated by MEA was the dominant factor and no obvious change of photocurrent exhibit. Thus 1:3 was finally selected as the optional volume ratio between Au NCs and MEA. Fig. 6B depicted the influence of the cyclic voltammetry to get optimal cycles of Glycine. The cycles were measured for 10, 15, 20, 25 and 30 respectively, and highest photocurrent response was emerged at 25 cycles, suggesting that the modified electrode have good electrochemical conductivity. Whereas, a slight reduction of peak photocurrent appeared at 30 cycles, thus, this phenomenon proved 25 cycles was the most compatible cycles. As for Fig. S6C, it can be found that the photocurrent increased rapidly with the concentration of RMC, while as RMC concentration exceeds 3mg/mL, the photocurrent showed downward trend

gradually for excess RMC on electrode suppressed. Thus, 3mg/mL RMC was selected as the optimal concentration for immunoassay.

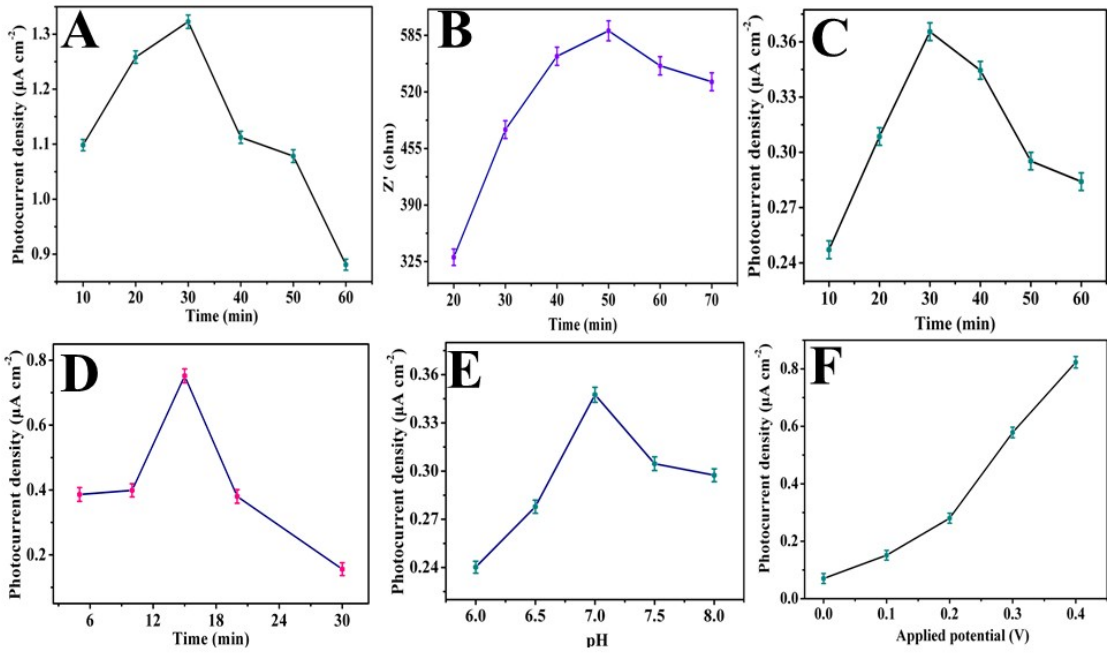

Figure S7 The effect of different (A) the absorption time between RMC and tyramine, (B) ZEN-MAb incubate time, (C) competitive reaction time between target free ZEN and peptide@Tyr-RMC conjugate, (D) HRP catalysis time (2 Mm H_2O_2 solution). (E) pH and (F) applied potential during the PEC measurement.

Fig. S7A evaluated the optimal absorption time between RMC and tyramine, owing to the self-oxidation of tyramine, the electron–hole recombination in RMC was suppressed which promote electron transfer efficiently. The photocurrent decreased when absorption time exceed 30 min due to the increased amount of tyramine hindered the transfer of electrons on the electrode interface. Therefore, the optimal response was obtained at 30 min. As Fig. S7B exhibited, the impedance increased with increasing ZEN-MAb incubation time and reached top at 50 min. The impedance decreased gradually when the incubation time was prolonged, which can be ascribed to the approximately saturated reaction between ZEN-MAb and poly(Gly). And the photocurrent output was mainly dependent capture amount of peptide@Tyr-RMC

conjugate on electrode, thus, the competitive reaction time between target free ZEN and peptide@Tyr-RMC conjugate was explored in Fig. S7C, the photocurrent response enhanced sharply from 10 to 30 min, and decreased when the time exceed 30 min for more insulated protein complex hindered the electron migration seriously. Fig. 7D presented the effect of HRP catalysis time on the photocurrent response after the electrode interface has been captured by peptide@Tyr-RMC conjugate in 2 mM H_2O_2 solution. The photocurrent response increased gradually from 6 to 15 min and decreased when further prolonging the catalysis time. There are mainly two factors: (i) aggregation of the Tyr-RMC conjugate made more electron-hole recombination (ii) with the increase of film thickness, the internal resistances increase, which led to decrease of photocurrent. The effect of pH variation on the photocurrent response was investigated in the range of 6-8. As exhibited in Figure S7E, the photocurrent density elevated rapidly and reached maximum at pH=7.0 and then decreased with increasing of the pH. Thus, pH 7.0 was selected as the optimum pH in the subsequent measurements. Besides, Figure S7F investigated the effect of applied potential on the photoelectrochemical response toward the detection of the ZEN from 0.0-0.4V, with the increase of positive potential, the photocurrent increased sharply resulting from the lower electron-transfer energy barrier. However，in order to avoid oxidation of substrate in high positive potential, 0.2 V was selected as the applied potential during the determination progress.

S1 Y.M. Lin, Y. L. Su, Y. H. Zhu, Z. Y. Jiang, H.L. Shi, X. Ding, X. D. Zhang, H. Y. Zhu, R. Q. Zhang, Computational Materials Science., 2017,131,178.